HHS Public Access

Author manuscript

Bone. Author manuscript; available in PMC 2019 September 01.

Published in final edited form as:

Bone. 2018 September ; 114: 22–31. doi:10.1016/j.bone.2018.06.002.

Reversal of loss of bone mass in old mice treated with mefloquine

Rafael Pacheco-Costa[1,*], **Hannah M. Davis**[1,*], **Emily G. Atkinson**[1], **Julian E. Dilley**[1], **Innocent Byiringiro**[1], **Mohammad W. Aref**[1], **Matthew R. Allen**[1,2], **Teresita Bellido**[1,2,3], and **Lilian I. Plotkin**[1,2]

[1]Department of Anatomy & Cell Biology, Indiana University School of Medicine, Indianapolis, IN 46202, USA

[2]Roudebush Veterans Administration Medical Center, Indianapolis, IN 46202, USA

[3]Division of Endocrinology, Department of Internal Medicine, Indiana University School of Medicine, Indianapolis, IN 46202, USA

Summary

Aging is accompanied by imbalanced bone remodeling, elevated osteocyte apoptosis, and decreased bone mass and mechanical properties; and improved pharmacologic approaches to counteract bone deterioration with aging are needed. We examined herein the effect of mefloquine, a drug used to treat malaria and systemic lupus erythematosus and shown to ameliorate bone loss in glucocorticoid-treated patients, on bone mass and mechanical properties in young and old mice. Young 3.5-month-old and old 21-month-old female C57BL/6 mice received daily injections of 5mg/kg/day mefloquine for 14 days. Aging resulted in the expected changes in bone volume and mechanical properties. In old mice mefloquine administration reversed the lower vertebral cancellous bone volume and bone formation; and had modest effects on cortical bone volume, thickness, and moment of inertia. Mefloquine administration did not change the levels of the circulating bone formation markers P1NP or alkaline phosphatase, whereas levels of the resorption marker CTX showed trends towards increase with mefloquine treatment. In addition, and as expected, aging bones exhibited an accumulation of active caspase3-expressing osteocytes and higher expression of apoptosis-related genes compared to young mice, which were not altered by mefloquine administration at either age. In young animals, mefloquine induced higher periosteal bone formation, but lower endocortical bone formation. Further, osteoclast numbers were higher

[*]Corresponding author: Lilian I. Plotkin, Ph.D., Department of Anatomy and Cell Biology, Indiana University School of Medicine, 635 Barnhill Drive, MS-5035, Indianapolis, IN 46202-5120. Phone: 1-317-274-5317. Fax: 1-317-278-2040. lplotkin@iupui.edu.
[*]RPC and HMD contributed equally to this work.

Declarations of interest: none

Author contributions

Study design was performed by RPC and LIP. Data acquisition was performed by RPC, HMD, EGA, JED, IB, and MWA. Advice on μCT analysis and biomechanical testing was performed by MRA. Data analysis and interpretation was performed by RPC, HMD, TB, and LIP. Drafting of manuscript was performed by RPC, HMD, and LIP. All authors revised the manuscript and approved the final version.

on the endocortical bone surface and circulating CTX levels were increased, in mefloquine-compared to vehicle-treated young mice. Consistent with this, addition of mefloquine to bone marrow cells isolated from young mice led to increased osteoclastic gene expression and a tendency towards increased osteoclast numbers *in vitro*. Taken together our findings identify the age and bone-site specific skeletal effects of mefloquine. Further, our results highlight a beneficial effect of mefloquine administration on vertebral cancellous bone mass in old animals, raising the possibility of using this pharmacologic inhibitor to preserve skeletal health with aging.

Keywords

cell/tissue signaling; osteoclast; aging; therapeutics

Introduction

A combination of intrinsic factors, including elevated oxidative stress, increased endogenous glucocorticoid action and low sex steroids [1], and reduced physical activity, lead to bone loss and increased risk of fractures with advanced age. This not only results in considerable morbidity, but also elevated mortality following, for example, hip fractures [2]. As the skeleton ages, there is an imbalance in bone remodeling with bone resorption prevailing over bone formation, resulting in a net loss of bone mass [3]. In addition, bone mechanical properties decrease with aging. Factors associated with aging, have opposite effects on osteoclasts and osteoblasts, resulting in increased differentiation/activity of the bone resorbing cells whereas bone forming cells exhibit increased apoptosis and reduced activity. Osteocyte apoptosis and empty lacunae are also increased with aging and their accumulation is associated with defective bone material properties [4, 5]. Further, osteoclasts accumulate in areas nearby apoptotic osteocytes, but not in the vicinity of empty lacunae, suggesting that dying osteocytes secrete factors that signal for osteoclast recruitment [6–11].

Mefloquine is a member of the quinine-derived family of drugs that also includes chloroquine and hydroxychloroquine, commonly used in patients to treat malaria and systemic lupus erythematosus [12]. As a group, the quinine-derived family of drugs are inhibitors of autophagy [13]. In addition, it has been shown that mefloquine inhibits membrane channels such as pannexin 1 (Panx1) [14, 15], L-type calcium channels [16], potassium channels [17], volume-regulated and calcium-activated chloride channels [18], ATP-sensitive potassium channels [19], and connexin channels [20]. Studies in patients have shown that hydroxychloroquine administration results in attenuated spinal bone loss when the drug is administered alongside glucocorticoids [21], an agent that induces bone loss and increases fragility [22]. Additionally, quinine-derived drugs increased spinal and hip bone mineral density in patients with systemic lupus erythematosus [23, 24]. Studies have shown that chloroquine reduces osteoclast numbers in young growing rodents and prevents overiectomy-induced bone loss in older, 8–9-month-old mice [25]. Whether this kind of drug alters the consequences of aging on the skeleton was heretofore unknown.

We hypothesized that by reducing osteoclast numbers mefloquine would ameliorate the deleterious skeletal effects of aging. To test this, we treated young and old mice with

mefloquine daily for 2 weeks. Unexpectedly, we found that short-term mefloquine administration did not decrease osteoclastogenesis in old mice and actually increased osteoclast number/activity in young mice. Further, in aged mice mefloquine increased vertebral cancellous bone formation and mass in a sclerostin-independent manner. In addition, our results suggest that mefloquine administration might prevent the consequences of aging on bone strength. These findings raise the possibility of using this pharmacologic inhibitor to improve the cancellous bone mass and strength with aging.

Materials and Methods

Mice and treatment

3.5-(young, n=8–9/group) and 21-month-old (old, n=10/group) C57BL/6 female mice were obtained from National Institute on Aging (NIA) and administered daily intraperitoneal injection of vehicle (1.5% ethanol) or 5mg/kg/day of mefloquine (BioBlocks Inc., San Diego, CA, USA, cat.# QU024-1) for 14 days [26]. Mice were assigned an ID number and the age and treatment were recorded in a database. Investigators performing endpoint measurements were only given the mouse IDs, thus blinded to treatment and age. Mice were randomized and assigned to each experimental group based on matching spinal BMD. Animals were sacrificed 4–6 hours after receiving the last injection. Mice (5/cage) were fed a regular diet (Envigo, Indianapolis, IN) and water *ad libitum*, and maintained on a 12h light/dark cycle. All experiments were carried out as planned, with no adverse effects resulting from treatments. The mice received intraperitoneal injections of calcein (30 mg/kg; Sigma-Aldrich, Saint Louis, MO, USA) and alizarin red (50 mg/kg; Sigma) 7 and 2 days before sacrifice, respectively, to allow for dynamic histomorphometric measurements [27].

Micro-computed tomography (μCT) analysis

Lumbar vertebrae (L4) and femora were dissected, cleaned of soft tissue and wrapped in PBS-soaked gauze and frozen at −20°C until imaging [28]. Bones were scanned using 50kV source, 120mA, 151milliseconds integration time, and 10μm voxel resolution on a μCT-35 (Scanco Medical AG, Brüttisellen, Switzerland). Scans were reconstructed and analyzed using manufacturer software. The following parameters were obtained for the cancellous bone of the lumbar vertebrae: trabecular bone volume per total volume (BV/TV, %), trabecular number (Tb.N, mm-1), trabecular thickness (Tb.Th, mm), and trabecular spacing (Tb.Sp, mm). For cortical bone of the femoral diaphysis, the following parameters were obtained: bone area/total area (%), marrow cavity area (mm^2), cortical thickness (mm), and polar moment of inertia (Ip, mm4). Nomenclature is reported in accordance with suggested guidelines for μCT [29].

Bone histomorphometry

Lumbar vertebrae (L1–L3) and femora and were dissected and fixed in 10% neutral buffered formalin [28]. Dynamic histomorphometric analysis of unstained methyl methacrylate embedded L1–L3 vertebra longitudinal sections, avoiding the primary spongiosa, and femoral mid-diaphysis cross-sections was performed using an epifluorescence microscope. Static histomorphometric analysis was performed on decalcified, paraffin-embedded femoral mid-diaphysis cross-sections (for osteoclasts) and undecalcified plastic-embedded L1–L3

vertebra longitudinal sections (for osteoclasts and osteoblasts). Sections were stained for TRAP/Toluidine blue and von Kossa/McNeal in order to visualize osteoclasts and osteoblasts, respectively. Histomorphometric analysis was performed using the OsteoMeasure high resolution digital video system (OsteoMetrics Inc., Decatur, GA, USA). The terminology and units used are those recommended by the Histomorphometry Nomenclature Committee of the American Society for Bone and Mineral Research (ASBMR) [29].

Biomechanical testing

Three-point bending testing of the femoral mid-diaphysis was performed following previously published protocols [30]. Briefly, bones were thawed to room temperature, hydrated in 0.9% saline, and loaded to failure at 2mm/min with force versus displacement data collected at 10Hz using a servo-hydraulic test system (TestResources Inc., Shakopee, MN, USA). Femora were loaded to failure in an anterior–posterior direction with the upper contact area at the mid-diaphysis (50% total bone length) and the bottom contact points centered around this point and separated by 8mm. Whole bone mechanical properties (load, displacement, stiffness, energy) were derived from the load-displacement curves. Cross-sectional moment of inertia and anterior–posterior diameter were determined by μCT and were used to calculate estimated material-level properties, as previously described [30].

Immunohistochemistry for active caspase-3

Decalcified, paraffin-embedded femoral mid-diaphysis cross-sections were deparaffinized, treated with 3% H_2O_2 to inhibit endogenous peroxidase activity, blocked and then incubated with rabbit monoclonal anti-active caspase-3 antibody (1:75; Thermo Fisher Scientific In., Rockford, IL, USA, cat.#PA5-23921)[31]. Sections were then incubated with anti-rabbit biotinylated secondary antibody followed by avidin conjugated peroxidase (Vectastain Elite ABC Kit; Vector Laboratories Inc., Burlingame, CA, USA). Color was developed with a diaminobenzidine substrate chromogen system (Acros Organics, New Jersey, USA). Cells expressing the protein of interest are stained in brown, whereas negative cells are green-blue. Nonimmune IgG was used as a negative control. One section from each mouse at 400× magnification was evaluated.

RNA extraction and real-time PCR (qPCR)

Total RNA was isolated using TRIzol (Invitrogen, Grand Island, NY, USA), as previously published [32]. Reverse transcription was performed using a high-capacity cDNA kit (Applied Biosystems, Foster City, CA, USA). qPCR was performed using the Gene Expression Assay Mix TaqMan Universal Master Mix and an ABI 7900HT real-time PCR system. The housekeeping gene glyceraldehyde 3-phosphate dehydrogenase (GAPDH) was used. Primers and probes were commercially available (Applied Biosystems, Foster City, CA, USA) or were designed using the Assay Design Center (Roche Applied Science, Indianapolis, IN, USA). Relative expression was calculated using the ΔCt method [33].

Circulating bone markers

Blood was collected in vials containing the anti-coagulant BD SST by cheek bleeding after 4 hours of fasting. Plasma was separated, aliquoted, and stored at −80°C until used [30]. Plasma N-terminal propeptide of type I procollagen (P1NP) (Immunodiagnostic Systems Inc., Fountain Hill, AZ, USA, cat.#AC-33F1) and C-telopeptide fragments (CTX) (RatLaps, Immunodiagnostic Systems Inc., Fountain Hill, AZ, USA, cat.#AC-06F1) were measured as described by the manufacturer. Alkaline phosphatase activity was assessed by a standard automated method using a Randox Daytona chemical analyzer (Randox Laboratories Ltd., Crumlin, United Kingdom).

Osteoclastogenesis assay

Non-adherent bone marrow cells (3×10^5 cells/cm^2) were plated on a 24-well with 20ng/ml recombinant murine M-CSF and 80ng/ml recombinant murine soluble RANKL (PeproTech Inc., Rocky Hill, NJ, USA) with either 1mM of mefloquine or vehicle. Medium was changed every 2 days for 7 days [28]. The conditioned medium (CM) was collected at day 7 to measure ATP concentration. Osteoclasts exhibiting 3 or more nuclei were enumerated after staining for TRAPase using a commercial kit (Sigma-Aldrich, Saint Louis, MO, USA, cat.#387A). Images were acquired using a Zeiss Axiovert 35 microscope equipped with a digital camera (Carl Zeiss, Thronwood, NY, USA). mRNA was isolated from parallel cultures and gene expression was measured by qPCR (Applied Biosystems, Foster City, CA, USA).

Protein extraction and sclerostin measurement

Whole protein extracts from bone were prepared as published [11, 34]. Sclerostin levels were measured using an ELISA kit (R&D Systems, Inc., Minneapolis, MN, USA, cat.#MSST00) following the manufacturer instructions.

ATP staining

For ATP staining, cells were incubated with 100μM of quinacrine (Santa Cruz Biotechnology, Santa Cruz, CA, USA, cat.#sc-204222) in PBS for 20 min at 37% and 5% CO_2, rinsed twice with PBS. Images were immediately taken using a fluorescence microscope. Cells were then lysed and 10μl of each sample were mixed with 100μl of luciferin-luciferase reagent in a 96-well black clear-bottom microplate and luminescence was measured. Values are expressed as relative light units (RLU).

Statistical analysis

Data were analyzed by using SigmaPlot 13.0 (Systat Software Inc., San Jose, CA, USA). All values are reported as the mean ± standard deviation. Differences among samples were analyzed by two-way ANOVA, with post-hoc analysis using Tukey test or by t-test, as appropriate. Differences were considered significant when $p \leq 0.05$.

Study approval

The protocols involving animal procedures were approved by the Institutional Animal Care and Use Committee of Indiana University School of Medicine.

Results

Mefloquine administration reverses vertebral cancellous bone loss in old mice

Vertebral bone volume/tissue volume (BV/TV) was significantly lower in vehicle-treated old compared to young mice (Fig. 1). Mefloquine treatment reversed the low BV/TV in old mice through significant effects on trabecular thickness, without affecting young animals. Trabecular number was not altered by either age or treatment. The changes in vertebral cancellous bone were accompanied by corresponding changes in bone formation rate (Fig. 2A). In old mice, bone formation was lower compared to young mice due to lower mineral apposition rate, whereas mineralizing surface, as well as osteoblast number were not changed (Fig. 2A and 2B). Mefloquine administration increased MAR and BFR in old mice (Fig. 2A). Further, osteoblast number was increased in both young and old animals treated with the drug (Fig. 2B), whereas the prevalence of apoptotic osteoblasts was not changed by administering mefloquine (not shown). On the other hand, osteoclast parameters were not changed with either age or pharmacologic treatment (Fig. 2C). This evidence suggests that increased vertebral cancellous bone in old mice treated with mefloquine is due to increased osteoblast activity.

Mefloquine shows tendencies towards improved mechanical properties but has minimal effects on the geometry of cortical bone in old mice

Microarchitecture analysis in the femoral mid-diaphysis of vehicle-treated old mice showed a reduction in cortical bone area/tissue area (BA/TA) and cortical thickness, while marrow cavity area, material density, moment of inertia, and tissue area (not shown) were higher when compared to young mice (Fig. 3). Mefloquine treatment induced a small but significant reduction in marrow cavity area and moment of inertia in old mice, without affecting cortical bone geometry in young animals.

Consistent with the alterations in femoral cortical bone architecture, skeletal aging had deleterious effects on the biomechanical properties of the femur as evidenced by decreased displacement to yield, yield stress, strain to yield, and resilience in vehicle-treated old mice (Table 1 and 2). Mefloquine administration differentially affected the mechanical properties in the two age groups. In young mice, mefloquine treatment had no effect on the mechanical or material properties, except for increasing toughness compared to vehicle-treated age-matched mice. On the other hand, in old mice, mefloquine treatment showed a tendency to reverse several parameters back to the levels observed in young vehicle-treated mice. Specifically, the structural property displacement to yield and several material properties, yield stress, strain to yield, and resilience, were not different in old mefloquine-treated mice compared to young vehicle-treated animals by post hoc statistical analysis, although the increases in these parameters did not reach significance when comparing old mice treated with the vehicle versus the drug.

Mefloquine administration alters femoral mid-diaphysis cortical bone turnover in young animals, without affecting these parameters in old mice

Dynamic histomorphometry on the periosteal surface of the femoral mid-diaphysis revealed higher mineral apposition rate, mineralizing surface and bone formation rate in vehicle-

treated old compared to young mice (Fig. 4A). On the other hand, mineralizing surface and bone formation rate were reduced (without changes in mineral apposition rate) on the endocortical surface in old mice. In old mice, mefloquine treatment had no effect on the bone formation parameters on either the periosteal or endocortical surface. On the other hand, pharmacological treatment in young mice resulted in increased bone formation parameters on the periosteal surface, whereas endocortical mineralizing surface and bone formation were reduced. Osteoclast number and surface on the endocortical bone were not changed by age, but were significantly increased with mefloquine treatment in young and not old mice (Fig. 4B).

No changes in the circulating markers of bone resorption or formation were detected in old compared to young mice, although a tendency towards increased in alkaline phosphatase was found in vehicle-treated old mice ($p= 0.055$) (Fig. 5A). Consistent with the increase in cortical osteoclasts observed in young treated animals, mefloquine administration increased the levels of the resorption marker C-terminal telopeptide (CTX) in the circulation of young, but not old mice. On the other hand, the levels of the bone formation markers procollagen I intact N-terminal (P1NP) and alkaline phosphatase (ALP) did not change with mefloquine administration. The lack of effect of mefloquine on circulating bone formation markers could be due to the fact that osteoblast activity was changed in some, but not all bone compartments.

Mefloquine treatment increased osteoclast differentiation *in vitro*

We next examined the effect of mefloquine *in vitro* and found that treatment of non-adherent bone marrow cells with the drug led to a tendency towards increased osteoclast number without changes in size; and a significant increase in the expression of TRAP and calcitonin receptor in the mature osteoclasts (Fig. 5A and B). Similar effects were obtained when mefloquine was removed from the media after 5 days of culture, but not when the drug was added 5 days after starting osteoclast differentiation (not shown), suggesting that mefloquine has an effect on osteoclast precursors and not in mature cells. However, we cannot exclude the possibility that mefloquine increases osteoclast differentiation by acting indirectly on stromal cells that might be present in the non-adherent bone marrow cell cultures.

Mefloquine has been shown to inhibit the opening of pannexin1 channels [14, 15, 26] and to prevent ATP release [35, 36]. Consistent with this, mature osteoclast cultures exhibited more intracellular ATP in the presence of mefloquine (Fig. 5C). The change in ATP levels was not associated with dysregulation of pannexin levels, as aging or mefloquine treatment did not alter Panx1 or 3 levels and Panx2 was only detected in some, but not all bone samples (not shown).

Mefloquine administration increases the prevalence of empty lacunae and reduces Sost levels in young but not old mice

In order to investigate the mechanism behind increased bone mass in old mefloquine-treated mice, levels of Sost/sclerostin, a potent bone formation inhibitor, were measured. Despite the increased mRNA levels of the Sost gene measured in the marrow-flushed tibia samples compared to vehicle-treated young mice, sclerostin expression was lower in vertebra bone

lysates of vehicle-treated old mice (Fig. 6A and B). These results are consistent with the increases in the total number of osteocytes, potentially expressing sclerostin, in the cortical bone of the femur, while a reduction in the total number of osteocytes was observed in vertebral cancellous bone of old compared to young vehicle-treated mice (Fig. 6C). Mefloquine treatment reduced Sost mRNA without affect sclerostin protein levels in young mice, and did not affect Sost/sclerostin expression in old animals. On the other hand, while osteocyte number was increased in the old mice, the proportion of apoptotic osteocytes, determined by active caspase-3 staining, and number of empty osteocyte lacunae was increased in old compared to young mice in both treatment groups (Fig. 6D). Further, mRNA levels of several apoptosis markers were increased in marrow-flushed tibia samples from the old animals (Fig. 6E). In old mice, mefloquine treatment did not alter osteocyte apoptosis or apoptotic gene expression in the cortical bone of the femoral mid-diaphysis, whereas in young mice a tendency towards increase in the number of caspase-3 positive osteocytes and a significant increase in the number of empty lacunae were observed with drug treatment. Our evidence suggests the possibility that the higher periosteal bone formation in femur of young mefloquine treated mice and old mice from both treatment groups, could be due to a local decrease in sclerostin levels in bone resulting from a decrease in the number of sclerostin-expressing osteocytes.

Discussion

In this study, we found that short-term administration of mefloquine, a quinine-derived drug, shown to ameliorate the adverse skeletal effects of glucocorticoids and lupus [21, 23, 24], differentially effects bone formation in a bone site and age-specific manner. In old mice, it increases vertebral cancellous bone formation leading to increases in cancellous bone mass. Whereas in young mice while it increases bone formation on the periosteal surface of the femoral mid-diaphysis, it decreases endocortical bone formation. In addition, we found that mefloquine increases the number of osteoclasts on the endocortical surface of the femur and the circulating CTX levels only in young animals. Further, bone mechanical properties showed tendencies towards increase following mefloquine administration in old, but not young mice.

The mechanism(s) by which mefloquine exerted these effects is not clear, as the drug is able to affect several channels. In particular, it has previously been shown that the drug blocks Panx1 channels in the nervous system [26] and acts on these channels with high sensitivity [14, 15]. Pannexins are a recently discovered class of single-membrane channel forming proteins that share similar topology with connexin channels, but do not form gap junctions [37]. This small family of integral membrane proteins consists of three members, Panx1, Panx2, and Panx3, with approximately 94% similarity between mice and humans [38]. Pannexins have a distinct pattern of expression. Panx1 is the most well-characterized and widely expressed pannexin family member [39]. Panx2 was originally believed to only be expressed in the nervous system, but has recently been found in other tissues [40], including osteoblasts in bone [41]. Panx3 is expressed in bone, teeth, and skin [39].

Panx1 channels open in apoptotic cells as a result of cleavage of the Panx1 auto-inhibitory domain by active caspase-3 [35, 36]. This leads to the release of ATP, which functions as a

"find-me" chemotactic signal for phagocytes. Thus, opening of Panx1 channels in apoptotic osteocytes could result in ATP release and osteoclast differentiation through direct actions on osteoclast precursors and indirectly by stimulating RANKL expression in osteoclastogenesis supporting cells [42, 43]. Consistent with this possibility, global deletion of Panx1 inhibited osteoclast recruitment in apoptotic osteocyte-containing bone regions where mechanically-induced microdamage had occurred [44]. However, in this study mefloquine treatment did not alter osteoclastogenesis in the old mice, and actually increased femur endocortical osteoclast number/surface in the young mice. This increase could result from direct effects of mefloquine on osteoclastic cells, as suggested by our *in vitro* findings demonstrating an increase in osteoclast differentiation in the presence of mefloquine. Unlike our findings on osteoclast differentiation, it was demonstrated that an analog, chloroquine, prevents osteoclastogenesis by suppressing canonical and non-canonical NF-κB signaling [25]. Furthermore, disruption for nuclear mitochondrial transcription factor A (*Tfam)* gene reduced intracellular ATP in osteoclasts and led to a decrease in osteoclast survival [45]. In our study, upon mefloquine treatment *in vitro*, osteoclasts accumulated intracellular ATP, which might have prolonged their lifespan. Future studies are needed to examine the role of ATP on mefloquine effects in osteoclasts.

In addition to pannexin, mefloquine can also inhibit other channels, such as cardiac L-type calcium channels [16] and potassium channels [17], volume-regulated and calcium-activated chloride channels in pulmonary artery endothelial cells [18], ATP-sensitive potassium channels in pancreatic β cells [19], and N2A neuroblastoma cell Cx36 channels (and Cx50, Cx43, Cx32, and Cx26 at higher concentrations) [20]. These inhibitory effects of mefloquine are exerted at concentrations between 1–100μM, with EC_{50} ranging between 0.3 and 3μM. While no side-by-side comparison for the different receptors in the same cell type have been reported, the effects of mefloquine on pannexin channels can be detected at concentrations of 10–100nM, suggesting high sensitivity of pannexin channels to mefloquine effects. Nevertheless, we cannot exclude the possibility that the beneficial effects of mefloquine on the skeleton are due to inhibition of channels other than pannexins. Future studies will be performed to identify the molecular target for the effects of mefloquine on the skeleton.

Our findings demonstrate that mefloquine administration results in bone compartment- as well as age-dependent changes in bone cell differentiation/activity, bone mass and mechanical properties. Thus, in old animals mefloquine increased vertebral cancellous bone formation, explaining the reversal of the decreased bone volume in the old mice, but did not alter femoral cortical bone turnover. On the other hand in young mice mefloquine did not alter vertebral cancellous bone turnover, but had opposite effects on periosteal (increases) and endocortical (decreases) bone formation, leading to no net change in femoral cortical thickness. It is possible that the different response in the bone compartments and old versus young mice is due to the short duration (2 weeks) of treatment and that, given enough time, all bones/animals will respond in a similar fashion. Further, we cannot exclude the possibility that the differences observed in cancellous versus cortical bone are due to the fact that the cancellous bone was analyzed in vertebral bone whereas the cortical bone was studied in femoral bone. In particular, it is possible that the difference in loading between the two bones influences the effect of aging and/or the drug. However, we have previously shown that similar effects can be seen in cancellous bone of the vertebra and the distal

femur, suggesting that the difference in responses are due to the difference in the compartment, rather than a difference in the loading of the bone [28, 30, 46].

Overall, we did not find any substantial changes in cortical bone structure following 2-week mefloquine administration, with only slight reductions in marrow cavity volume and moment of inertia, suggesting that the short-term administration of the drug was not enough to alter bone geometry. Nevertheless, we found that the drug showed tendencies towards increase, without reaching significance, on several bone biomechanical properties suggesting that bone quality might have improved in mice treated with mefloquine. Given the fact that mice were given the drug for only 2 weeks, it is possible that a longer duration of mefloquine administration may yield stronger effects on the structural and mechanical properties of the cortical bone in old mice. Further studies are needed to understand the basis of the improved mechanical properties.

Bone formation was increased in mice receiving mefloquine and, since mefloquine is known to be an inhibitor of several membrane channels, our evidence suggests that the target of mefloquine action is a repressor of osteoblast activity. Unlike our findings, a study by Boyce's group [25] using chloroquine at the same dose as the one used by us, did not find alterations in bone formation in 6-week-old mice or in osteoblastic cells *in vitro*. An increased sensitivity to the drugs with aging or the fact that the study by Boyce's group use a similar, but not identical drug could be the reason for the inconsistent outcomes.

Given the importance of Sost/sclerostin in the regulation of bone mass, we sought to determine whether the mechanism behind the increased bone formation in our experimental model involved changes in the expression of this protein. We found that sclerostin protein levels in bone were not affected by mefloquine treatment, suggesting that increased bone formation in mefloquine-treated mice is not due to downregulation of sclerostin levels. The mechanism of the increased bone formation with mefloquine warrants further investigation.

In summary, we show for the first time that mefloquine administration increases cancellous bone formation and volume in the vertebra and has beneficial effects on cortical bone mechanical properties in old mice. Our studies bring to light a potent pharmacological agent able to reverse at least partially the deleterious consequences of aging in bone.

Acknowledgments

This research was supported by the National Institutes of Health R01-AR053643 to LIP. The authors thank Padmini Deosthale for technical support. RPC received a scholarship from Coordination of Improvement of Higher Level Personnel (CAPES), Brazil (PDE# 232636/2014-1). EGA received a scholarship from IUPUI, Life-Health Sciences Internship Program and the CTSI - Clinical and Transitional Sciences Institute Award and JED from Ruth L. Kirschstein NRSA Short-Term Institutional Research Training Grant (NRSA) through the NIH (#4T35HL 110854-05). HMD and MWA are supported by an NIH T32-AR065971 grant. MWA was supported by NIH F30 DK115162 and NIH T32 AR065971.

References

1Manolagas SC. From Estrogen-Centric to Aging and Oxidative Stress: A Revised Perspective of the Pathogenesis of Osteoporosis. Endocr Rev. 2010; 31:266–300. [PubMed: 20051526]

2Cauley JA. Public health impact of osteoporosis. J Gerontol A Biol Sci Med Sci. 2013; 68:1243–1251. [PubMed: 23902935]

3Plotkin LI, Laird DW, Amedee J. Role of connexins and pannexins during ontogeny, regeneration, and pathologies of bone. BMC Cell Biology. 2016; 17:29–38. [PubMed: 27421907]

4Bivi N, Nelson MT, Faillace ME, Li J, Miller LM, Plotkin LI. Deletion of Cx43 from osteocytes results in defective bone material properties but does not decrease extrinsic strength in cortical bone. Calcif Tissue Int. 2012; 91:215–224. DOI: 10.1007/s00223-012-9628-z [PubMed: 22865265]

5Davis HM, Aref MW, Aguilar-Perez A, Pacheco-Costa R, Allen K, Valdez S, Herrera C, Atkinson EG, Mohammad A, Lopez D, Harris MA, Harris SE, Alen M, Bellido T, Plotkin LI. Cx43 overexpression in osteocytes prevents osteocyte apoptosis and preserves cortical bone quality in aging mice. JBMR Plus. 2018

6Aguirre JI, Plotkin LI, Stewart SA, Weinstein RS, Parfitt AM, Manolagas SC, Bellido T. Osteocyte apoptosis is induced by weightlessness in mice and precedes osteoclast recruitment and bone loss. J Bone Min Res. 2006; 21:605–615.

7Cardoso L, Herman BC, Verborgt O, Laudier D, Majeska RJ, Schaffler MB. Osteocyte apoptosis controls activation of intracortical resorption in response to bone fatigue. J Bone Miner Res. 2009; 24:597–605. [PubMed: 19049324]

8Emerton KB, Hu B, Woo AA, Sinofsky A, Hernandez C, Majeska RJ, Jepsen KJ, Schaffler MB. Osteocyte apoptosis and control of bone resorption following ovariectomy in mice. Bone. 2009; 46:577–583. [PubMed: 19925896]

9Tatsumi S, Ishii K, Amizuka N, Li M, Kobayashi T, Kohno K, Ito M, Takeshita S, Ikeda K. Targeted ablation of osteocytes induces osteoporosis with defective mechanotransduction. Cell Metab. 2007; 5:464–475. [PubMed: 17550781]

10Verborgt O, Gibson G, Schaffler MB. Loss of osteocyte integrity in association with microdamage and bone remodeling after fatigue in vivo. J Bone Min Res. 2000; 15:60–67.

11Bivi N, Condon KW, Allen MR, Farlow N, Passeri G, Brun L, Rhee Y, Bellido T, Plotkin LI. Cell autonomous requirement of connexin 43 for osteocyte survival: consequences for endocortical resorption and periosteal bone formation. J Bone Min Res. 2012; 27:374–389. DOI: 10.1002/jbmr.548

12Dahl G. ATP release through pannexon channels. Philos Trans R Soc Lond B Biol Sci. 2015:370.

13Golden EB, Cho HY, Hofman FM, Louie SG, Schonthal AH, Chen TC. Quinoline-based antimalarial drugs: a novel class of autophagy inhibitors. Neurosurg Focus. 2015; 38:E12.

14Iglesias R, Spray DC, Scemes E. Mefloquine blockade of Pannexin1 currents: resolution of a conflict. Cell Commun Adhes. 2009; 16:131–137. [PubMed: 20218915]

15Dahl G, Qiu F, Wang J. The bizarre pharmacology of the ATP release channel pannexin1. Neuropharmacology. 2013; 75:583–593. [PubMed: 23499662]

16Coker SJ, Batey AJ, Lightbown ID, Diaz ME, Eisner DA. Effects of mefloquine on cardiac contractility and electrical activity in vivo, in isolated cardiac preparations, and in single ventricular myocytes. Br J Pharmacol. 2000; 129:323–330. [PubMed: 10694239]

17Kang J, Chen XL, Wang L, Rampe D. Interactions of the antimalarial drug mefloquine with the human cardiac potassium channels KvLQT1/minK and HERG. J Pharmacol Exp Ther. 2001; 299:290–296. [PubMed: 11561091]

18Maertens C, Wei L, Droogmans G, Nilius B. Inhibition of volume-regulated and calcium-activated chloride channels by the antimalarial mefloquine. J Pharmacol Exp Ther. 2000; 295:29–36. [PubMed: 10991957]

19Gribble FM, Davis TM, Higham CE, Clark A, Ashcroft FM. The antimalarial agent mefloquine inhibits ATP-sensitive K-channels. Br J Pharmacol. 2000; 131:756–760. [PubMed: 11030725]

20Cruikshank SJ, Hopperstad M, Younger M, Connors BW, Spray DC, Srinivas M. Potent block of Cx36 and Cx50 gap junction channels by mefloquine. Proc Natl Acad Sci U S A. 2004; 101:12364–12369. [PubMed: 15297615]

21Mok CC, Mak A, Ma KM. Bone mineral density in postmenopausal Chinese patients with systemic lupus erythematosus. Lupus. 2005; 14:106–112. [PubMed: 15751814]

22Plotkin LI, Bellido T. Osteocytic signalling pathways as therapeutic targets for bone fragility. Nat Rev Endocrinol. 2016; 12:593–605. [PubMed: 27230951]

23Lakshminarayanan S, Walsh S, Mohanraj M, Rothfield N. Factors associated with low bone mineral density in female patients with systemic lupus erythematosus. J Rheumatol. 2001; 28:102–108. [PubMed: 11196509]

24Ruiz-Irastorza G, Ramos-Casals M, Brito-Zeron P, Khamashta MA. Clinical efficacy and side effects of antimalarials in systemic lupus erythematosus: a systematic review. Ann Rheum Dis. 2010; 69:20–28. [PubMed: 19103632]

25Xiu Y, Xu H, Zhao C, Li J, Morita Y, Yao Z, Xing L, Boyce BF. Chloroquine reduces osteoclastogenesis in murine osteoporosis by preventing TRAF3 degradation. J Clin Invest. 2014; 124:297–310. [PubMed: 24316970]

26Lutz SE, Gonzalez-Fernandez E, Ventura JC, Perez-Samartin A, Tarassishin L, Negoro H, Patel NK, Suadicani SO, Lee SC, Matute C, Scemes E. Contribution of pannexin1 to experimental autoimmune encephalomyelitis. PLoS ONE. 2013; 8:e66657. [PubMed: 23885286]

27Bivi N, Pacheco-Costa R, Brun LR, Murphy TR, Farlow NR, Robling AG, Bellido T, Plotkin LI. Absence of Cx43 selectively from osteocytes enhances responsiveness to mechanical force in mice. J Orthop Res. 2013; 31:1075–1081. DOI: 10.1002/jor.22341 [PubMed: 23483620]

28Pacheco-Costa R, Hassan I, Reginato RD, Davis HM, Bruzzaniti A, Allen MR, Plotkin LI. High Bone Mass in Mice Lacking Cx37 Due to Defective Osteoclast Differentiation. J Biol Chem. 2014; 289:8508–8520. DOI: 10.1074/jbc.M113.529735 [PubMed: 24509854]

29Dempster DW, Compston JE, Drezner MK, Glorieux FH, Kanis JA, Malluche H, Meunier PJ, Ott SM, Recker RR, Parfitt AM. Standardized nomenclature, symbols, and units for bone histomorphometry: A 2012 update of the report of the ASBMR Histomorphometry Nomenclature Committee. J Bone Miner Res. 2013; 28:2–17. DOI: 10.1002/jbmr.1805 [PubMed: 23197339]

30Pacheco-Costa R, Davis HM, Sorenson C, Hon MC, Hassan I, Reginato RD, Allen MR, Bellido T, Plotkin LI. Defective cancellous bone structure and abnormal response to PTH in cortical bone of mice lacking Cx43 cytoplasmic C-terminus domain. Bone. 2015; 81:632–643. [PubMed: 26409319]

31Delgado-Calle J, Anderson J, Cregor MD, Hiasa M, Chirgwin JM, Carlesso N, Yoneda T, Mohammad KS, Plotkin LI, Roodman GD, Bellido T. Bidirectional Notch signaling and osteocyte-derived factors in the bone marrow microenvironment promote tumor cell proliferation and bone destruction in multiple myeloma. Cancer Res. 2016; 76:1089–1100. [PubMed: 26833121]

32Davis HM, Pacheco-Costa R, Atkinson EG, Brun LR, Gortazar AR, Harris J, Hiasa M, Bolarinwa SA, Yoneda T, Ivan M, Bruzzaniti A, Bellido T, Plotkin LI. Disruption of the Cx43/miR21 pathway leads to osteocyte apoptosis and increased osteoclastogenesis with aging. Aging Cell. 2017; 16:551–563. [PubMed: 28317237]

33Livak KJ, Schmittgen TD. Analysis of relative gene expression data using real-time quantitative PCR and the $2^{-\Delta\Delta CT}$ method. Methods. 2001; 25:402–408. [PubMed: 11846609]

34Plotkin LI, Bivi N, Bellido T. A bisphosphonate that does not affect osteoclasts prevents osteoblast and osteocyte apoptosis and the loss of bone strength induced by glucocorticoids in mice. Bone. 2011; 49:122–127. DOI: 10.1016/j.bone.2010.08.011 [PubMed: 20736091]

35Sandilos JK, Chiu YH, Chekeni FB, Armstrong AJ, Walk SF, Ravichandran KS, Bayliss DA. Pannexin 1, an ATP release channel, is activated by caspase cleavage of its pore-associated C-terminal autoinhibitory region. J Biol Chem. 2012; 287:11303–11311. [PubMed: 22311983]

36Chiu YH, Jin X, Medina CB, Leonhardt SA, Kiessling V, Bennett BC, Shu S, Tamm LK, Yeager M, Ravichandran KS, Bayliss DA. A quantized mechanism for activation of pannexin channels. Nat Commun. 2017; 8:14324. [PubMed: 28134257]

37Panchin Y, Kelmanson I, Matz M, Lukyanov K, Usman N, Lukyanov S. A ubiquitous family of putative gap junction molecules. Curr Biol. 2000; 10:R473–R474. [PubMed: 10898987]

38Penuela S, Bhalla R, Nag K, Laird DW. Glycosylation regulates pannexin intermixing and cellular localization. Mol Biol Cell. 2009; 20:4313–4323. [PubMed: 19692571]

39Penuela S, Harland L, Simek J, Laird DW. Pannexin channels and their links to human disease. Biochem J. 2014; 461:371–381. DOI: 10.1042/BJ20140447 [PubMed: 25008946]

40Le Vasseur M, Lelowski J, Bechberger JF, Sin WC, Naus CC. Pannexin 2 protein expression is not restricted to the CNS. Front Cell Neurosci. 2014; 8:392.doi: 10.3389/fncel.2014.00392 [PubMed: 25505382]

41Xiao Z, Camalier CE, Nagashima K, Chan KC, Lucas DA, de la Cruz MJ, Gignac M, Lockett S, Issaq HJ, Veenstra TD, Conrads TP, Beck GR Jr. Analysis of the extracellular matrix vesicle proteome in mineralizing osteoblasts. J Cell Physiol. 2007; 210:325–335. DOI: 10.1002/jcp.20826 [PubMed: 17096383]

42Buckley KA, Hipskind RA, Gartland A, Bowler WB, Gallagher JA. Adenosine triphosphate stimulates human osteoclast activity via upregulation of osteoblast-expressed receptor activator of nuclear factor-kappa B ligand. Bone. 2002; 31:582–590. [PubMed: 12477572]

43Rumney RM, Wang N, Agrawal A, Gartland A. Purinergic signalling in bone. Front Endocrinol (Lausanne). 2012; 3:116. [PubMed: 23049524]

44Cheung WY, Fritton JC, Morgan SA, Seref-Ferlengez Z, Basta-Pljakic J, Thi MM, Suadicani SO, Spray DC, Majeska RJ, Schaffler MB. Pannexin-1 and P2X7-Receptor Are Required for Apoptotic Osteocytes in Fatigued Bone to Trigger RANKL Production in Neighboring Bystander Osteocytes. J Bone Miner Res. 2016; 31:890–899. [PubMed: 26553756]

45Miyazaki T, Iwasawa M, Nakashima T, Mori S, Shigemoto K, Nakamura H, Katagiri H, Takayanagi H, Tanaka S. Intracellular and extracellular ATP coordinately regulate the inverse correlation between osteoclast survival and bone resorption. J Biol Chem. 2012; 287:37808–37823. [PubMed: 22988253]

46Delgado-Calle J, Tu X, Pacheco-Costa R, McAndrews K, Edwards R, Pellegrini G, Kuhlenschmidt K, Olivos N, Robling A, Peacock M, Plotkin LI, Bellido T. Control of bone anabolism in response to mechanical loading and PTH by distinct mechanisms downstream of the PTH receptor. J Bone Miner Res. 2017; 32:522–535. [PubMed: 27704638]

Highlights

- Aging is accompanied by imbalanced bone remodeling, elevated osteocyte apoptosis, and low bone mass/strength and new effective therapies are needed.
- Mefloquine effect was tested in young 3.5-month-old and old 21-month-old mice.
- Mefloquine increases vertebral cancellous bone formation and volume and has beneficial effects on cortical bone mechanical properties in old mice.
- Mefloquine is a potent pharmacological agent able to reverse at least partially the deleterious consequences of aging in bone.

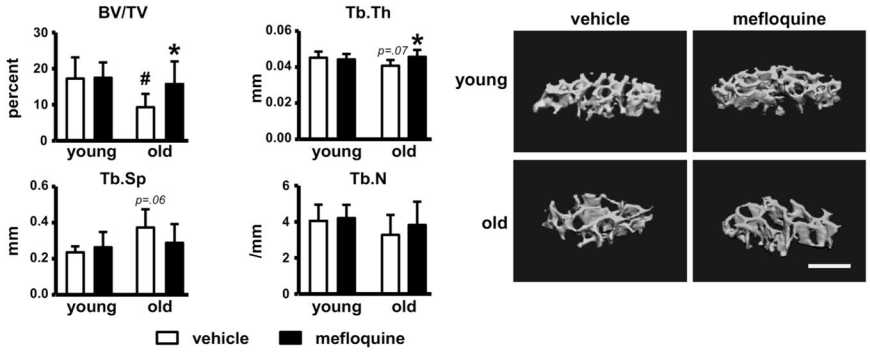

Fig. 1. Deleterious effect of aging on bone mass is partially reversed by mefloquine administration

(A) Cancellous bone microarchitecture analysis in L4 vertebra was assessed by μCT in mefloquine-treated young and old mice (n=6–10). Representative 3D images of cancellous bone in vertebra are shown. Bars represent mean ± s.d., $^{\#}p<0.05$ versus vehicle-treated young mice; *p<0.05 versus vehicle treated mice at the same age, by two-way ANOVA. All scale bars indicate 500μm.

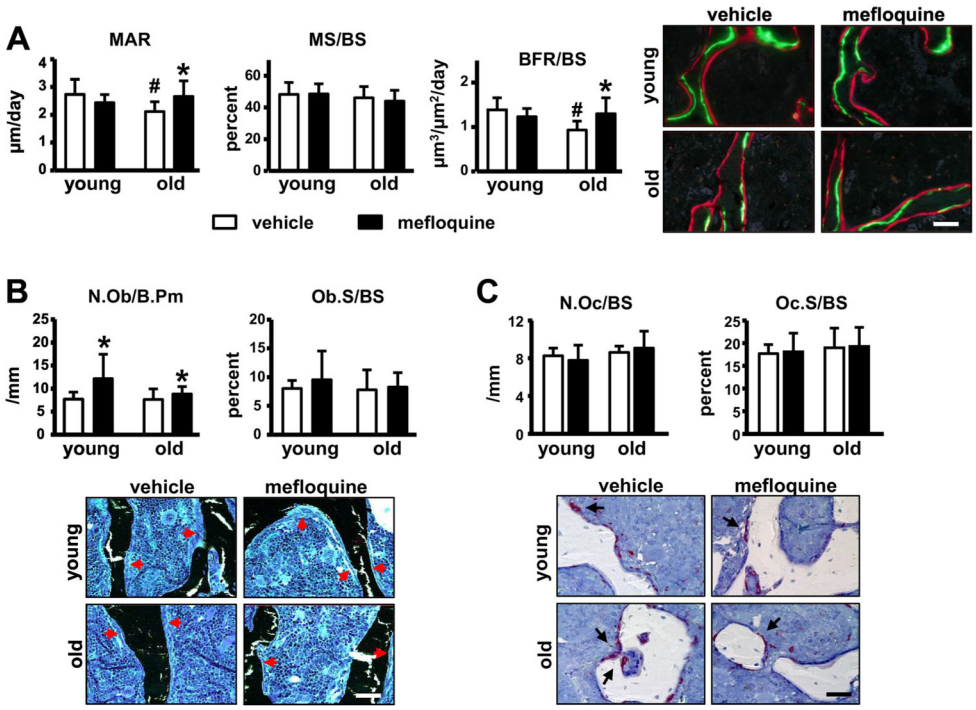

Fig. 2. Mefloquine administration reverses the decrease in bone formation induced by aging

(A) MAR, MS/BS, and BFR/BS were measure in unstained sections of lumbar vertebra (n=7–10). **(B)** N.Ob/BS and Ob.S/BS were scored in lumbar vertebra stained with von Kossa/McNeal (n=7–10). **(C)** N.Oc/BS, Oc.S/BS, and ES/BS were scored in lumbar vertebra stained for TRAPase/Toluidine blue (n=7–8) in young and old mice. Bars represent mean ± s.d., #p<0.05 versus vehicle-treated young mice; *p<0.05 versus vehicle treated mice at the same age, by two-way ANOVA. Representative images from lumbar vertebra sections for the corresponding analysis are shown (red arrows; osteoblasts and black arrows; osteoclasts). All scale bars indicate 50µm.

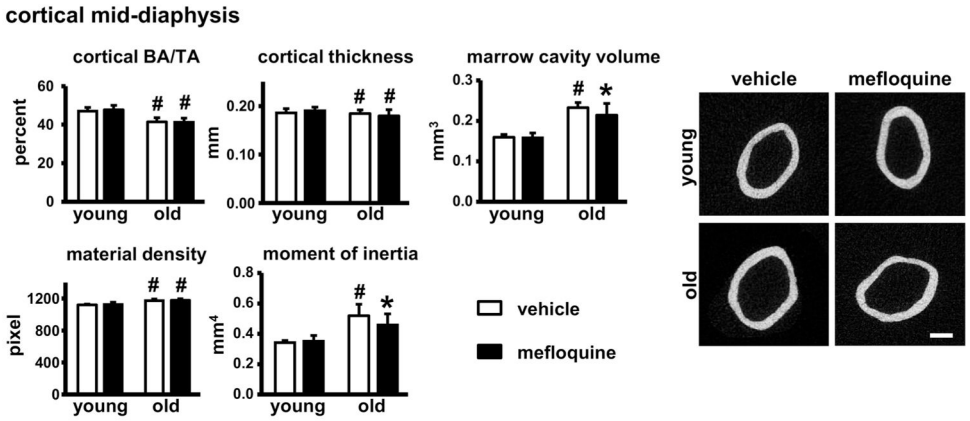

Fig. 3. Administration of mefloquine has minimal effects on cortical bone geometry

Cortical bone geometry in the femoral mid-diaphysis was assessed by μCT (n=6–10) in young and old mice. Representative cross-section images of femoral mid-diaphysis are shown. Bars represent mean ± s.d., $^{\#}p<0.05$ versus vehicle-treated young mice; *p<0.05 versus vehicle treated mice at the same age, by two-way ANOVA. All scale bars indicate 500μm.

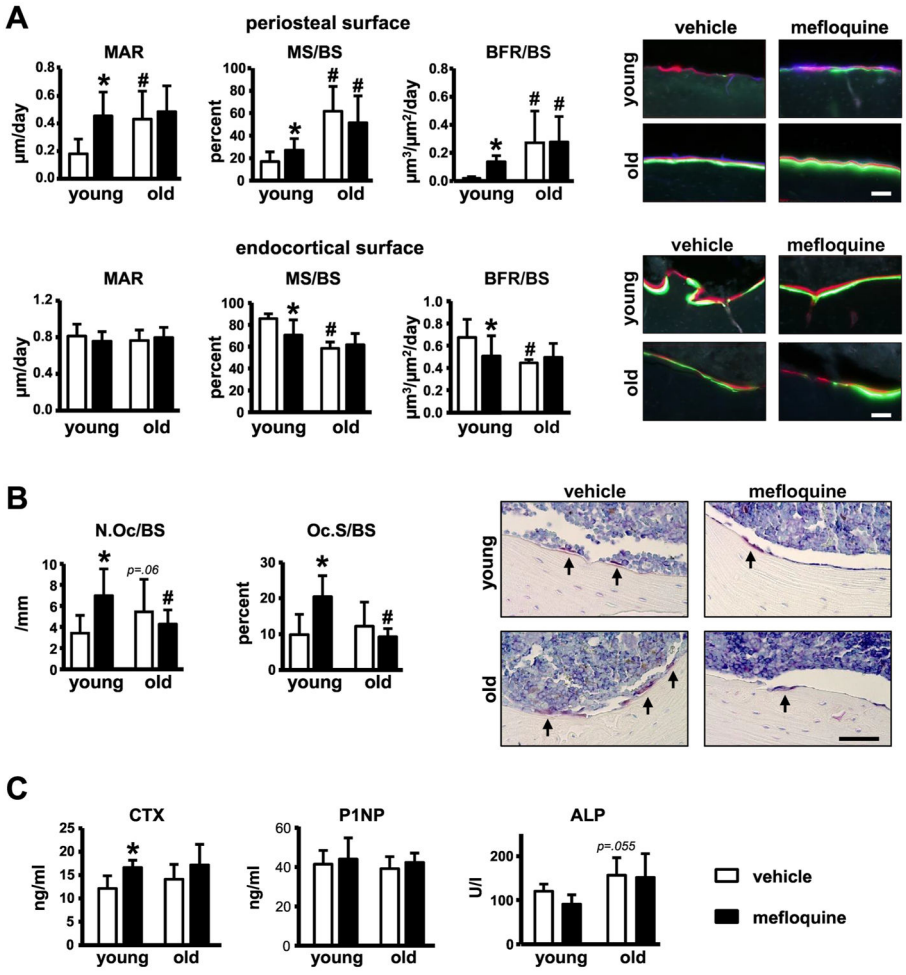

Fig. 4. Mefloquine-treated young, but not old mice exhibit changes in histomorphometric parameters in cortical bone

(A) MAR, MS/BS, and BFR/BS were measured in unstained sections of femoral mid-diaphysis (n=6–9). **(B)** N.Oc/BS, Oc.S/BS, and ES/BS were measured in cross-section of femoral mid-diaphysis stained for TRAPase (n=7–10). Representative images from osteoclasts on the bone surface (arrow, magenta) are shown. **(C)** Markers of bone resorption and formation were measured in serum from young and old mice treated with vehicle or mefloquine (n=6–10). Bars represent mean ± s.d., $^{\#}p<0.05$ versus vehicle-treated young mice; *p<0.05 versus vehicle treated mice at the same age, by two-way ANOVA. All scale bars indicate 50μm.

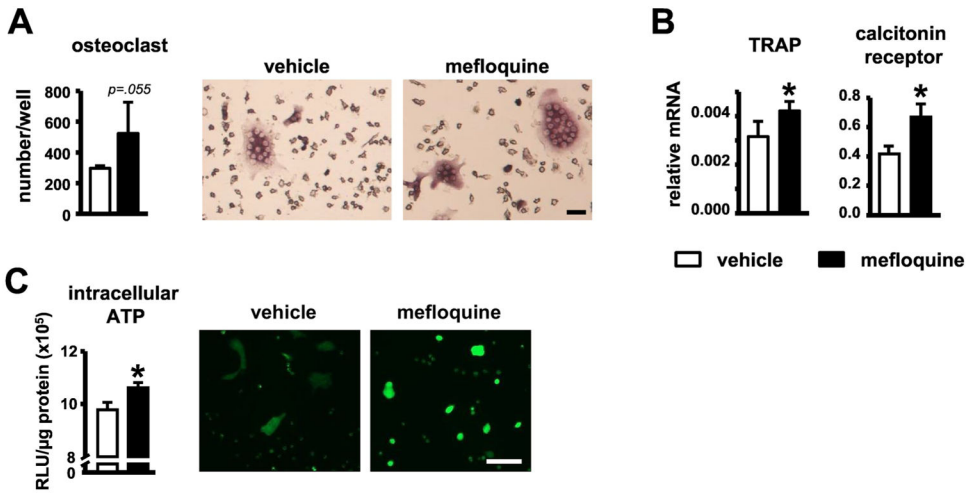

Fig. 5. Increased serum bone resorption markers in young and old mice, and osteoclast differentiation *in vitro* induced by mefloquine

(**A**) Osteoclast number and (**B**) genes associated with osteoclast differentiation in cultures of non-adherent bone marrow cells treated with M-CSF and sRANKL, measured by qPCR and corrected by GAPDH (n=4). Representative images of *in vitro* generated osteoclasts are shown. Scale bars indicate 10µm. (**C**) ATP levels were measured in osteoclast lysates (intracellular ATP, n=3) after 7 days of differentiation using a luciferin-luciferase kit. Mature osteoclasts treated with vehicle or 1mM mefloquine for 24h were stained using 100µM quinacrine and visualized under fluorescence microscope (n=3). Scale bars indicate 100µm. Bars represent mean ± s.d. *p<0.05 versus vehicle treated group, by t-test.

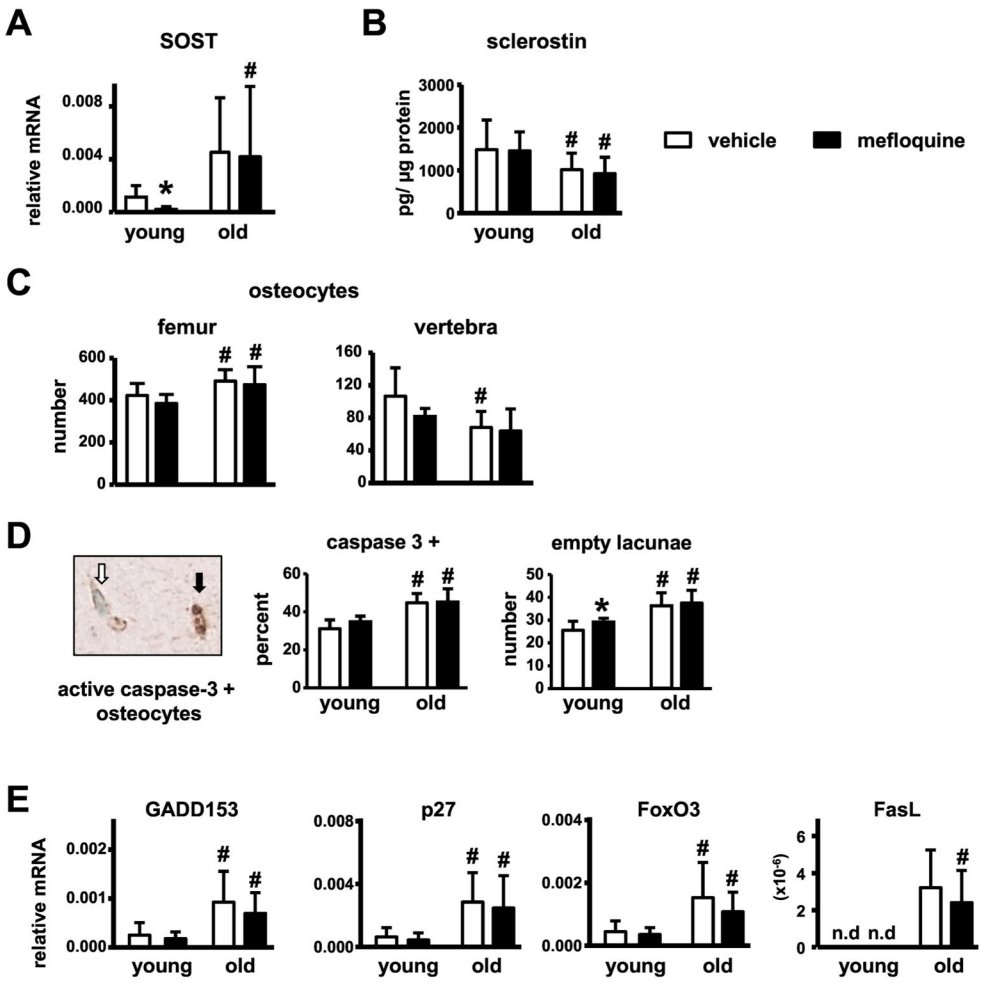

Fig. 6. Mefloquine administration does not affect sclerostin levels or osteocyte apoptosis in young or old mice

(A) Sost mRNA was measured in mefloquine-treated young and old mice in tibia (n=8–10). (**B**) sclerostin protein levels were measured by ELISA in L5 vertebra lysates (n=8–10). (**C**) Osteocyte numbers were measured in cortical bone of the femur and cancellous bone of the L3 vertebra (n=8–10). **(D)** Apoptotic osteocytes (active caspase-3-positive) and empty lacunae were enumerated in the femoral mid-diaphysis of young and old mice (n=5–9). Representative immunostaining image with a typical active caspase-3-positive (black arrow, brown) and viable osteocyte (white arrow, blue-green) is shown. **(E)** Genes associated with apoptosis were measured in tibiae without bone marrow cells at 3.5 and 21 months of age by qPCR and corrected by GAPDH (n=6–10).

Table 1

Biomechanical structural properties are altered in mefloquine-treated mice.

Structural properties						
	young + vehicle	**young + mefloquine**	**old + vehicle**	**old + mefloquine**	**p value (two-way ANOVA)**	
Yield force (N)	11.59 ± 2.11	10.71 ± 1.68	9.47 ± 4.25	11.19 ± 2.02	age treatment age × treatment	0.411 0.667 0.197
Ultimate force (N)	16.57 ± 3.09	15.03 ± 1.57	19.85 ± 4.59	17.61 ± 4.61	age treatment age × treatment	0.031 0.153 0.787
Displacement to yield (μm)	142.49 ± 36.86	142.12 ± 23.45	**94.70 ± 22.23**	122.23 ± 46.56	age treatment age × treatment	0.007 0.250 0.238
Postyield displacement (μm)	484.88 ± 303.07	706.76 ± 394.22	380.83 ± 217.01	418.99 ± 195.36	age treatment age × treatment	0.071 0.223 0.386
Total displacement (μm)	627.37 ± 307.50	848.88 ± 393.39	475.53 ± 208.39	593.33 ± 190.75	age treatment age × treatment	0.059 0.113 0.621
Stiffness (N/mm)	105.23 ± 25.58	89.80 ± 19.57	115.01 ± 37.86	121.63 ± 37.50	age treatment age × treatment	0.070 0.693 0.327
Work to yield (mJ)	0.85 ± 0.28	0.83 ± 0.19	0.56 ± 0.27	0.79 ± 0.41	age treatment age × treatment	0.131 0.312 0.224
Postyield work (mJ)	5.94 ± 2.19	8.17 ± 3.40	5.59 ± 2.74	6.31 ± 3.13	age treatment	0.298 0.167

Structural properties						
	young + vehicle	**young + mefloquine**	**old + vehicle**	**old + mefloquine**	**p value (two-way ANOVA)**	
					age × treatment	0.474
Total work (mJ)	6.78 ± 2.22	9.00 ± 3.36	6.14 ± 2.66	6.61 ± 3.11	age	0.147
					treatment	0.198
					age × treatment	0.396

Bolded values $p<0.05$ vs. vehicle-treated young mice, by post hoc analysis (n=7–9/treatment group).

Table 2

Biomechanical material properties are altered in mefloquine-treated mice.

Material properties						
	young + vehicle	**young + mefloquine**	**old + vehicle**	**old + mefloquine**	**p value (two-way ANOVA)**	
Yield stress (MPa)	55.31 ± 16.37	55.19 ± 13.19	**30.33 ± 14.07**	41.54 ± 8.89	age treatment age × treatment	<0.001 0.263 0.253
Ultimate stress (MPa)	77.45 ± 17.17	78.27 ± 19.68	66.06 ± 9.73	71.30 ± 22.91	age treatment age × treatment	0.165 0.641 0.734
Strain to yield (με)	15580 ± 3745	16745 ± 3195	**11136 ± 3164**	13843 ± 3802	age treatment age × treatment	0.006 0.126 0.535
Total strain (με)	68060 ± 30545	101240 ± 50520	54416 ± 67592	67593 ± 32152	age treatment age × treatment	0.068 0.073 0.429
Modulus (GPa)	4.43 ± 1.05	3.86 ± 0.69	3.64 ± 1.26	4.05 ± 1.24	age treatment age × treatment	0.434 0.843 0.208
Resilience (MPa)	0.46 ± 0.22	0.51 ± 0.21	**0.20 ± 0.11**	0.35 ± 0.18	age treatment age × treatment	0.005 0.129 0.489
Toughness (MPa)	3.52 ± 1.44	5.66 ± 2.69 *	2.27 ± 1.25	3.72 ± 0.99	age treatment age × treatment	0.040 0.020 0.373

* p<0.05 vs. corresponding vehicle-treated mice, by two-way ANOVA, bolded values p<0.05 vs. vehicle-treated young mice, by post hoc analysis.